



Eco-Friendly Biosynthesis of Nanoparticles Employing Orange Peel Extract

Article Type: Research Article	Authors T. Manoj and K. Abid
Article publication history: Article Received on : 03-Aug-2025 Article Accepted on : 05-Sep-2025 Article Published on: 10-Sept-2025	Affiliation Department of Chemistry, University of Rajasthan, Jaipur-302 004 India
Article review details: ^{1st} Review By. Dr. P. S. Soni ^{2nd} Review By. Dr. J.K. Rajwani Final Recommendation By: Prof: Neetesh Pandey	Corresponding Email zutshiraj@gmail.com DOI: https://dx.doi.org/10.65979/ujc.8.3.12

Abstract

The ability of green nanotechnology to remove harmful chemicals while making the economical and efficient synthesis of desired products is making it increasingly important. The reduction of harmful heavy metals with aqueous plant extracts is a fast, economical, and environmentally friendly way to create nanoparticles. In this study, silver nanoparticles (AgNPs) were prepared through a chemical reduction process by using orange peel extracts and 1 mM silver nitrate (AgNO_3) solution. During the synthesis, orange peel extract acts as reducing agent as well as capping agent. Using UV-visible absorption spectroscopy, the resonance of surface plasmon phenomenon of AgNPs was found at 445 nm. Various physicochemical methods, such as Fourier transform infrared (FT-IR) spectroscopy, energy dispersive X-ray spectroscopy (EDS), transmission electron microscopy (TEM) and X-ray diffraction (XRD) were used to further characterize the biosynthesized AgNPs. Aldehydes were the main substances in charge of the successful production of AgNPs, according to GCMS spectrometry examination of the orange peel extract. In addition, the synthesized AgNPs displayed strong antibacterial activity against both Gram-positive (*Staphylococcus aureus*) and Gram-negative (*Escherichia coli*) microorganisms. This green synthesis method gives the added advantage of producing useful compounds from fruit waste that could have potential antibacterial activity.

Keywords Green nanotechnology, orange peel extract, FTIR, UV-Vis, antibacterial activity

Introduction

Nanotechnology primarily emphasizes the fabrication of nanoparticles (NPs) with controlled sizes, shapes, and physicochemical properties, aiming to harness their potential benefits for humanity (1,2). Among the rapidly evolving domains of nanotechnology is the synthesis of metal nanoparticles, typically ranging in size from 1 to 100 nanometers (nm).

When materials are reduced to the nanoscale, their intrinsic properties can significantly differ from those in bulk form. These unique characteristics make nanostructured materials suitable for diverse applications in fields such as bioengineering, medicine, and agriculture. Notably, nanoparticles are also well-known for their antibacterial and biocidal activities (3,4). Various techniques have been employed for nanoparticle synthesis, including chemical reduction methods (5), as well as electrochemical, photochemical (6,7), and physical approaches like physical vapor condensation (8). In recent years, green synthesis has emerged as a sustainable and eco-friendly strategy for nanoparticle production (9–11), involving the use of natural reducing agents such as sugars, vitamins, biodegradable polymers, microorganisms, and plant extracts (12).

The biosynthesis of silver nanoparticles (AgNPs) often involves the reduction of silver nitrate (AgNO_3) solutions using plant extracts. This process generally comprises two key stages:

Stage 1: Nucleation Phase – Individual silver atoms cluster together to form initial nuclei, requiring high activation energy.

Stage 2: Growth Phase – These nuclei subsequently grow into well-defined nanoparticles through aggregation and stabilization (13,14).

The properties of the resulting AgNPs are strongly influenced by the types of biomolecules present in the plant extracts used (15–17). Therefore, the choice of extract plays a critical role in nanoparticle synthesis, as it supplies bio-reductive compounds such as phenolic substances, flavonoids, terpenoids, alkaloids, polysaccharides, proteins, enzymes, and amino acids (18).

AgNPs synthesized via green methods are typically free from toxic contaminants, making them well-suited for medical and pharmaceutical applications (4–6). Additionally, silver-based antimicrobial packaging represents a promising form of active packaging that helps reduce microbial contamination and extends the shelf life of food products.

Despite the established use of AgNPs in food packaging due to their antimicrobial effects, there remain concerns about the potential leaching of silver ions (Ag^+) into food and beverages. These concerns have prompted stricter oversight by food safety regulatory agencies (7). Various plant extracts—such as those derived from *Murraya koenigii* leaves (8), mangosteen (9), *Mangifera indica* (10), *Jatropha curcas* (13), *Cinnamomum zeylanicum* (19), *Camellia sinensis* (20), *Aloe vera* (21), mushrooms (22), and honey (23)—have been explored in the green synthesis of AgNPs. Comparatively fewer studies have investigated the use of fruit extracts, including those from papaya (16), tansy (18), pear (23), lemon (24), and gooseberry (25). One advantage of using plant and fruit extracts is their ability to produce stable nanoparticles that

resist aggregation even during prolonged storage. However, most existing studies on AgNP synthesis using plant extracts focus on flora from Europe, Africa, the Americas, and parts of Asia. There remains a notable research gap in eco-friendly nanoparticle synthesis using fruit extracts, particularly from Northeast India (26).

Citrus sinensis (orange) is native to Southern China, Northeast India, and Myanmar, with historical references in Chinese literature dating back to 314 BC. Oranges are hybrids of mandarin and pomelo, with the latter serving as the maternal lineage. Globally cultivated for their sweet taste, oranges are mainly produced in Brazil, followed by China and India, with global production reaching approximately 76 million tons in 2022. Within India, states like Assam (3.34%), Arunachal Pradesh (1.08%), Madhya Pradesh (32.89%), Punjab, Maharashtra, Rajasthan, and Haryana contribute significantly to total production.

Typically, orange peels are discarded after the pulp is consumed. However, limited studies have explored the potential of orange peel extracts in AgNP synthesis (27,28). These peels are the primary byproduct of industrial citrus juice production, accounting for about 50–65% of the fruit's total weight. Rich in proteins, soluble and insoluble fibers, and bioflavonoids, this biomass holds significant promise for nanobiotechnological applications, especially in nanoparticle synthesis (29,30).

The present study aimed to explore the use of orange peels, readily available in Northeast India, as both reducing and capping agents for the biosynthesis of silver nanoparticles. The synthesized AgNPs were systematically characterized using various spectroscopic and microscopic techniques, including UV-Visible spectroscopy, Fourier-transform infrared spectroscopy (FTIR), transmission electron microscopy (TEM), energy-dispersive X-ray spectroscopy (EDS), and X-ray diffraction (XRD). Furthermore, the antibacterial efficacy of the synthesized AgNPs was evaluated against *Escherichia coli* and *Staphylococcus aureus*.

MATERIALS AND METHODS

Plant Material and Preparation of Extracts

Oranges were procured from a local market in Guwahati, Assam (coordinates: 19.47°N, 72.8°E) in October 2022. The fresh peels were thoroughly rinsed with double-distilled water and then shade-dried. Once dried, the peels were ground into powder. Ten grams of this powdered peel were subjected to reflux extraction in 100 mL of double-distilled water using a 500 mL beaker for one hour. The mixture was then filtered through Whatman No. 1 filter paper, and the resulting filtrate was collected and stored in a separate flask for further use.

Green Synthesis of Silver Nanoparticles (AgNPs)

The biosynthesis of silver nanoparticles was carried out using the aqueous orange peel extract and silver nitrate (AgNO_3) under sunlight, following the method reported by Rizwana et al. (31). A 1 mM aqueous solution of AgNO_3 was freshly prepared by dissolving the salt in 1000 mL of distilled water. To synthesize the AgNPs, 9 mL of the silver nitrate solution was mixed

with 1 mL of the orange peel extract. This mixture was then exposed to direct sunlight to facilitate the reduction process.

A noticeable color change from yellow to reddish-brown indicated the formation of silver nanoparticles, attributed to the surface plasmon resonance (SPR) effect. The formation of AgNPs was further confirmed by the presence of a characteristic absorption peak in the UV-visible spectrum.

Characterization Techniques

To monitor the reduction of silver ions over time, UV-Vis spectroscopy was employed using a Shimadzu UV spectrophotometer (Model UV-1240). The reaction mixture was slightly diluted, and spectra were recorded within a wavelength range of 200 to 800 nm. The integration time was set at 1 second, with 1 nm intervals between measurements.

Further structural characterization was performed using an Advanced Powder X-ray Diffractometer (Bruker D8, Germany), utilizing a Cu K α radiation source ($\lambda = 1.54056 \text{ \AA}$) at 40 kV and 40 mA. The scanning was conducted at a rate of 3°/minute over a 2 θ range from 5° to 100°.

For functional group analysis, a Perkin Elmer FTIR Spectrometer (Model FTIR System Spectrum BX) was used. The samples were prepared using the KBr pellet method, and spectra were collected in transmission mode over a range of 4000 to 400 cm⁻¹, with a resolution of 4 cm⁻¹.

Morphological analysis was carried out using Transmission Electron Microscopy (TEM) with a JEM-2100 PLUS (HR) system from JEOL, operating at 200 kV and equipped with an EDS (Energy Dispersive Spectroscopy) detector. A small drop of the sample was placed on carbon-coated copper grids and dried before analysis. Particle size distribution was determined from the TEM images using image analysis software.

The chemical constituents of the orange peel extract were identified using Gas Chromatography-Mass Spectrometry (GC-MS) on a Hewlett-Packard 6890 Plus gas chromatograph, coupled with a 5975 mass selective detector.

Antimicrobial Activity Assessment

The antibacterial efficacy of the synthesized AgNPs was tested against *Staphylococcus aureus* (Gram-positive) and *Escherichia coli* (Gram-negative) using the agar well diffusion method. Overnight cultures of the test organisms were evenly spread onto sterile nutrient agar plates.

Using a sterile cork borer, wells of 8 mm diameter were made in the solidified agar. A defined volume of AgNP solution was introduced into each well under sterile conditions. After

allowing a 15-minute pre-diffusion period at room temperature, the plates were incubated for 48 hours at $25 \pm 1^\circ\text{C}$.

Post-incubation, the antibacterial activity was evaluated by measuring the diameters of the inhibition zones around each well, indicating the effectiveness of the AgNPs against the respective bacterial strains.

RESULTS AND DISCUSSION

To synthesize silver nanoparticles (AgNPs) in an eco-friendly manner, orange peel extract was added to an aqueous solution of silver nitrate. A visible color change from yellowish to brown confirmed the successful formation of AgNPs, which is attributed to the excitation of surface plasmon vibrations. The biosynthesis of AgNPs was monitored using UV-Vis spectroscopy. Figure 1 illustrates the process of using orange peel extract for the green synthesis of silver nanoparticles. The observed color change validates the formation of AgNPs. In this method, the orange peel extract acts as a reducing agent, donating electrons to silver ions (Ag^+) in the aqueous solution and converting them into their zero-valent metallic form (Ag^0). This reduction initiates the nucleation and subsequent growth of colloidal AgNPs, which begin as small clusters. Several factors can influence the nucleation and growth of AgNPs, including reaction temperature, pH, precursor concentration, types of reducing and stabilizing agents, and the ratio of AgNO_3 to orange peel extract (32).



Fig.1: Change of colour from extract to nanoparticles

UV-Vis characterization

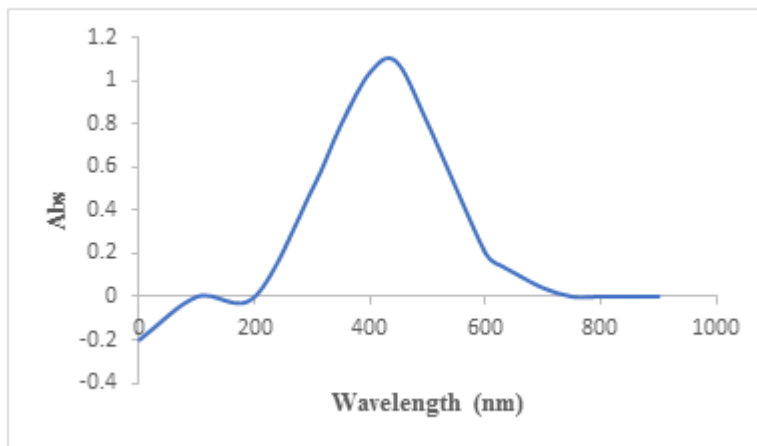


Fig. 2: UV-vis spectra of reduced Ag ions to AgNPs with orange peel extract.

Figure 2 presents the UV-Vis spectrum of silver nanoparticles (AgNPs) synthesized using orange peel extract. The absorption spectrum of the AgNPs displays a distinct peak at 445 nm within a broad wavelength range of 200 to 800 nm. This peak lies within the surface plasmon resonance (SPR) region of AgNPs, confirming their formation (33). Additionally, the broad plasmon band with an extended absorption tail at higher wavelengths (Figure 2) can be attributed to the size distribution of the biosynthesized AgNPs (34).

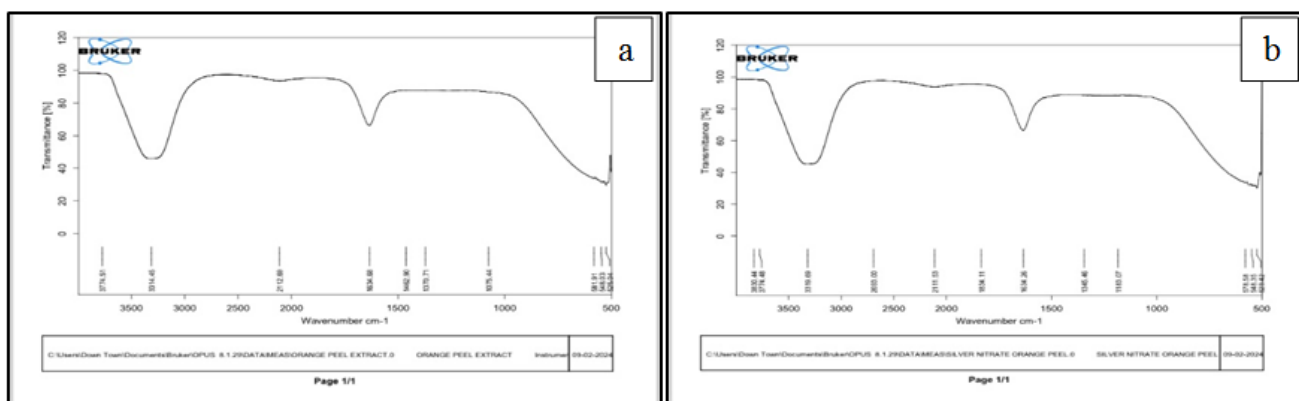


Fig. 3: (a) FTIR spectra of orange peel extract; (b) FTIR spectra of AgNPs

The extract's functional groups and their function in reducing AgNO_3 to generate AgNPs were investigated using FT-IR experiments (Fig. 3a-b). FT-IR spectrum of orange peel extract and colloidal AgNPs are similar with a slight shift in the positions of the bands.

(Shown in Fig.3a and 3b respectively). Peaks for AgNPs were found at 3319, 2111, 1634, 1345, 1183 cm^{-1} stretching vibration frequencies. For orange peel extract it were found at 3314, 2112, 1634, 1370, 1075 cm^{-1} stretching vibration frequencies. The extract's carboxylic groups and phenols' OH stretching vibrations are represented by the broad band at 3319 cm^{-1} . The phytoconstituents of the extract are thought to contain alkyne groups, which are responsible for the absorbance peak at 2111 cm^{-1} . The strong band at 1634 cm^{-1} corresponds to the C=C stretching of the aromatic ring. This stretch may be due to the C=O vibration of the ketones found in flavonoids. The peaks at 1183 and 1075 cm^{-1} are indicative of the C-N stretching vibrations of aliphatic amides (35).

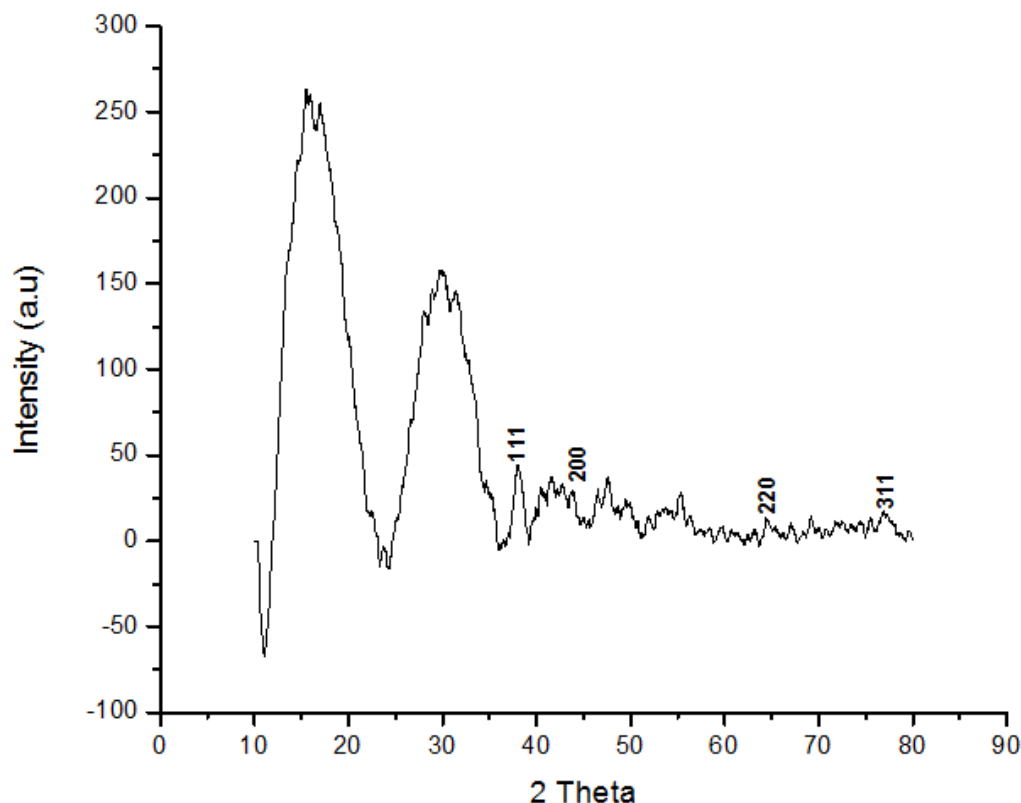


Fig. 4: XRD pattern of AgNPs by orange peel extract

Figure 4, the FCC (face-centered cubic) lattice structure of metallic silver is associated with the diffraction peaks at $2\theta = 37.2^\circ$, 44.08° , 64.44° , and 77.28° in the XRD pattern of the biosynthesized AgNPs. These peaks correspond to the (111), (200), (220), and (311) planes, respectively. Figure 4 shows additional peaks at $2\theta = 27.98^\circ$, 31.24° , 46.52° , 54.96° , 57.36° , and 76.92° , which are probably associated with the crystalline and amorphous organic phases that coexist with the crystallized AgNPs.

Further, information about the size and shape of the synthesized AgNPs was given by the TEM analysis. TEM images at various magnifications are shown in Figures 5 (a), (b) and (c) along with the selected area electron diffraction (SAED) patterns that are shown in Figure 5 (d).

The average diameter showed by the TEM images was about 8 to 20 nm which resembles the pattern observed in the SPR band of the UV-visible spectrum (36). Furthermore, as seen in Figure 5, it was revealed that the nanoparticles were evenly distributed and hardly aggregated.

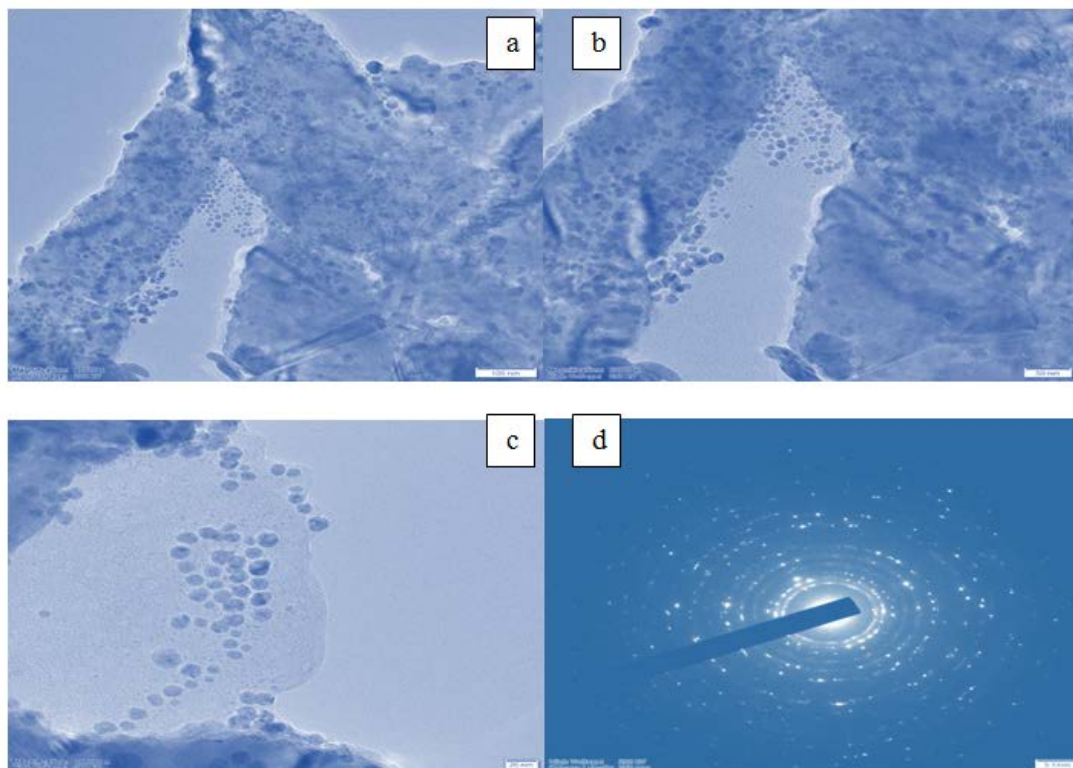


Fig. 5 : The images of AgNPs produced using orange peel extracts, which were captured by a transmission electron microscope (TEM), are: (a) a random field view of AgNPs (scale bar = 100 nm), (b) a high magnification image of spherical AgNPs (scale bar = 50 nm), (c) another high magnification image of spherical AgNPs (scale bar = 20 nm), and (d) the electron diffraction pattern (SAED) of several silver NPs.

The existence of AgNPs is confirmed by EDS microanalysis, as indicated in Figure 6 and gives chemical analysis of the constituents or composition at specific locations. The spectra identified elements such as O, C, Ag, and Au. Peaks from Cu and C came from the carbon grid that had been used to prepare the sample. FTIR analysis verifies that the double carbonyl groups in the sample are probably the origin of the elemental oxygen peak. AgNP production is confirmed by a signal in the silver portion of the spectrum. Surface plasmon resonance is linked to the optical absorption peak that metallic silver nanocrystals usually display at about 3 keV (37).

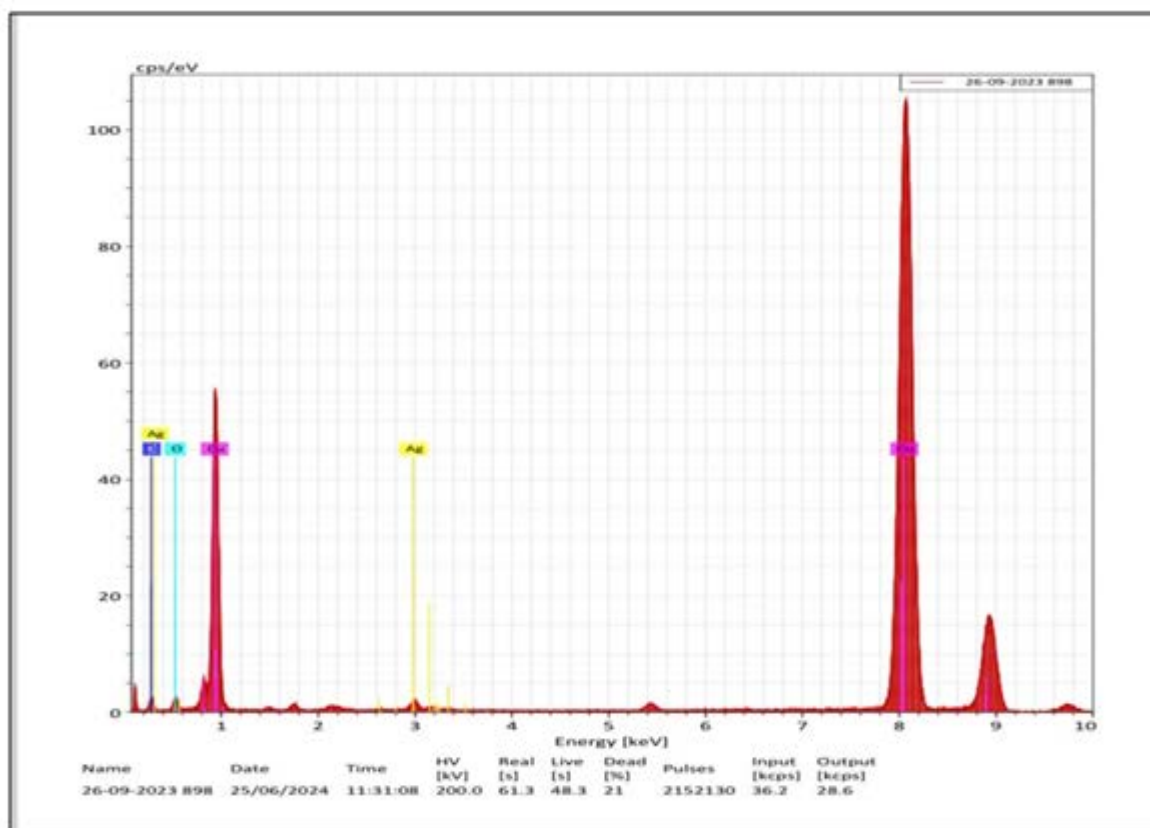


Fig. 6: Energy dispersion X-ray (EDS) spectra of AgNPs synthesized with *orange peel* extract

GC/MS analysis was done for orange peel extract of which the TIC diagram is given in Figure 7. In Table 2 the identified components along with retention time, compound names and area percentage are listed. Briefly, several compounds were found in the orange peel extract (5-Bromopentanoyl chloride, retention time (RT) 6.97 min) or were found in higher abundance in the orange peel extract (2(3H)-Furanone, 5- methyl-, RT 7.381 min; 2,6-dimethyl-2,6-octadiene-1,8-dial, RT20.33 min; and 4-isopropenyl- 1-methyl-1,2-cyclohexanedial, RT 20.92 min). Alcohols D-limonene (RT 10.123 min), β -linalool (RT 16.67 min), 1-nonanol (RT 17.98 min), 2-(4-methylenecyclohexyl)-2-propen-1-ol (RT 20.10 min), perilla alcohol (RT 20.25 min), and 8-hydroxylinalool (RT 21.03 min) were identified to exist in the higher amount from orange peel.

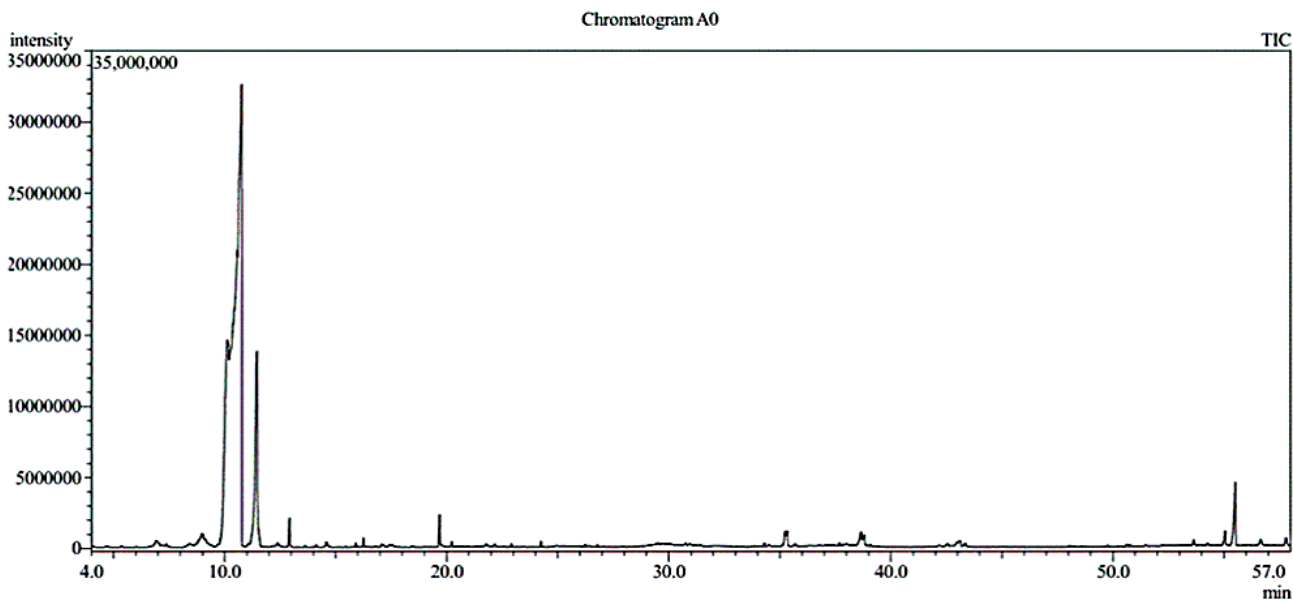


Fig. 7: GC/MS analysis of orange peel extract

Table 1-: Compounds present in orange peel extract

S. No.	RT. Time (min)	Compound name	Area Percentage
1	6.97	5-Bromopentanoyl chloride	0.25
2	6.915	.alpha.-Pinene	0.29
3	7.167	.beta.-Pinene	0.12
4	7.381	2(3H)-Furanone, 5-methyl-	0.14
4	8.972	.beta.-Myrcene	1.39
5	9.145	.beta.-Myrcene	0.31
6	9.27	Pentanoic acid, 4-oxo-, methyl ester	0.21
7	10.123	D-Limonene	17.08
8	10.577	D-Limonene	33.46
9	10.764	D-Limonene	26.52
10	11.457	.gamma.-Terpinene	9.41
11	12.4	Cyclohexene, 1-methyl-4-(1-methylethylidene)-	0.19
12	12.929	Linalool	0.63
13	14.592	Citronellal	0.21
14	16.253	Decanal	0.16
15	19.685	2-Methoxy-4-vinylphenol	0.72
16	35.229	Dibutyl phthalate	0.41

17	38.656	Linoelaidic acid	0.59
18	38.799	9,12,15-Octadecatrienoic acid, (Z,Z,Z)-	0.35
19	42.558	3',4',5,6,7,8-Hexamethoxyflavone	0.15
20	42.995	3',4',5,6,7,8-Hexamethoxyflavone	0.18
21	43.119	3',4',5,6,7,8-Hexamethoxyflavone	0.12
22	43.347	3',4',5,6,7,8-Hexamethoxyflavone	0.13
23	53.633	4H-1-Benzopyran-4-one, 5-hydroxy-6,7-dimethoxy-2-(4-methoxyphenyl)-	0.16
24	55.056	5-O-Desmethyltangeretin	0.43
25	56.659	Stigmasterol	0.22
26	57.798	gamma.-Sitosterol	0.26
27	55.504	4',5,6,7,8-Pentamethoxyflavone	2.01



Fig. 8(a):*E. coli* **Fig. 8(b):** *S. aureus*

Antimicrobial Activity

The well-diffusion method was used to evaluate the antibacterial activity of orange peel-derived silver nanoparticles against Gram-negative *Escherichia coli* and Gram-positive *Staphylococcus aureus* bacteria (in Figures 8(a) and 8(b) respectively). The antibacterial activities of orange peel extract were also tested. AgNPs had inhibitory zones of 5 mm against *E. coli* and 7 mm against *S. aureus*. The values here represent the mean of three experimental trails. The inhibitory zone of AgNPs proved to be marginally more effective against the bacterial strains than the raw orange peel extract.

According to some theories, respiratory inhibition and eventual cell death are caused by interactions between silver nanoparticles and thiol groups of proteins on the cell membrane. Moreover, interactions between the cell wall and silver nanoparticles may improve membrane permeability by forming pits or pores, which would aid in the killing of bacteria (38).

Conclusion

The current work used extract of orange peel as a capping and reducing agent to produce a simple, economical, and environmentally acceptable method for the synthesis of AgNPs without using harmful or dangerous materials. A color change in the solution served as a visual indication of the synthesis of AgNPs. Further confirmation of the generation of AgNPs was obtained by using UV-Vis spectroscopy, where a surface plasmon absorption peak was observed at 466 nm in the UV-Vis spectrum. The FT-IR spectra of orange peel extract and colloidal AgNPs showed little difference as the location of the band was minor. In TEM images spherical or almost spherical nanoparticles with mean diameter between 8–20 nm could be observed. EDS analysis revealed considerable indications of the silver element in the nanoparticles confirming the fact that there existed silver content. The XRD pattern confirms that the biosynthesized AgNPs have a face-centered cubic crystalline structure. The biogenic AgNPs exhibited strong action against the *E. coli* and *S. aureus*. It may find interesting uses in hygiene and medicine by further researching on AgNPs synthesized using orange peel extract.

References:

1. Bhyan SB, Alam MM, Ali MS. Effect of Plant Extracts on Okra mosaic virus Incidence and Yield Related Parameters of Okra. *Asian J Agric Res.* 2007;1(3):112–8.
2. Sani Aliero A, Hasmoni SH, Haruna A, Isah M, Malek NANN, Ahmad Zawawi N. Bibliometric exploration of green synthesized silver nanoparticles for antibacterial activity. *Emerg Contam.* 2025;11(1).
3. Naddeo JJ, Ratti M, O'Malley SM, Gripenburg JC, Bubb DM, Klein EA. Antibacterial Properties of Nanoparticles: A Comparative Review of Chemically Synthesized and Laser-Generated Particles. *Adv Sci Eng Med.* 2015;7(12):1044–57.
4. Marin S, Vlasceanu G, Tiplea R, Bucur I, Lemnaru M, Marin M, et al. Applications and Toxicity of Silver Nanoparticles: A Recent Review. *Curr Top Med Chem.* 2015;15(16):1596–604.
5. Wang H, Qiao X, Chen J, Ding S. Preparation of silver nanoparticles by chemical reduction method. *Colloids Surfaces A Physicochem Eng Asp.* 2005;256(2–3):111–5.
6. Khaydarov RA, Khaydarov RR, Gapurova O, Estrin Y, Scheper T. Electrochemical method for the synthesis of silver nanoparticles. *J Nanoparticle Res.* 2009;11(5):1193–200.
7. Zaarour M, El Roz M, Dong B, Retoux R, Aad R, Cardin J, et al. Photochemical preparation of silver nanoparticles supported on zeolite crystals. *Langmuir.* 2014;30(21):6250–6.
8. Simchi A, Ahmadi R, Reihani SMS, Mahdavi A. Kinetics and mechanisms of nanoparticle formation and growth in vapor phase condensation process. *Mater Des.* 2007;28(3):850–6.

9. Veerasamy R, Xin TZ, Gunasagaran S, Xiang TFW, Yang EFC, Jeyakumar N, et al. Biosynthesis of silver nanoparticles using mangosteen leaf extract and evaluation of their antimicrobial activities. *J Saudi Chem Soc.* 2011;15(2):113–20.
10. Dubey SP, Dwivedi AD, Lahtinen M, Lee C, Kwon YN, Sillanpaa M. Protocol for development of various plants leaves extract in single-pot synthesis of metal nanoparticles. *Spectrochim Acta – Part A Mol Biomol Spectrosc.* 2013;103:134–42.
11. Fahim M, Shahzaib A, Nishat N, Jahan A, Bhat TA, Inam A. Green synthesis of silver nanoparticles: A comprehensive review of methods, influencing factors, and applications. *JCIS Open.* 2024;16.
12. Kharissova O V., Dias HVR, Kharisov BI, Pérez BO, Pérez VMJ. The greener synthesis of nanoparticles. *Trends Biotechnol.* 2013;31(4):240–8.
13. Mittal AK, Chisti Y, Banerjee UC. Synthesis of metallic nanoparticles using plant extracts. *Biotechnol Adv.* 2013;31(2):346–56.
14. Ale Y, Rana S, Nainwal N, Rawat S, Butola M, Zainul R, et al. Phytochemical Screening and Green Synthesis of Antibacterial Silver Nanoparticles of *Sapindus mukorossi* Fruit Extracts. *Res J Pharm Technol.* 2023;16(12):5643–9.
15. Harne S, Sharma A, Dhaygude M, Joglekar S, Kodam K, Hudlikar M. Novel route for rapid biosynthesis of copper nanoparticles using aqueous extract of *Calotropis procera* L. latex and their cytotoxicity on tumor cells. *Colloids Surfaces B Biointerfaces.* 2012;95:284–8.
16. Ramachandran R, Krishnaraj C, Stacey L, Soon Y, Thangavel K. Plant extract synthesized silver nanoparticles: An ongoing source of novel biocompatible materials. *Ind Crops Prod.* 2015;70:356–73.
17. Shaikh WA, Chakraborty S, Owens G, Islam RU. A review of the phytochemical mediated synthesis of AgNP (silver nanoparticle): the wonder particle of the past decade. *Appl Nanosci.* 2021;11(11):2625–60.
18. Rauwel E, Arya G, Praakle K, Rauwel P. Use of Aloe Vera Gel as Media to Assess Antimicrobial Activity and Development of Antimicrobial Nanocomposites. *Int J Mol Sci.* 2024;25(11).
19. Baker C.C, Pradhan A, Pakstis L, Pochan D.J, Shah S.I. Synthesis and Antibacterial Properties of Silver Nanoparticles. *J Nanosci Nanotechnol.* 2005;5:244–9.
20. Sánchez GR, Castilla CL, Gómez NB, García A, Marcos R, Carmona ER. Leaf extract from the endemic plant *Peumus boldus* as an effective bioproduct for the green synthesis of silver nanoparticles. *Mater Lett.* 2016;183:255–60.

21. Tajbakhsh M, Alinezhad H, Nasrollahzadeh M, Kamali TA. Green synthesis of the Ag/HZSM-5 nanocomposite by using *Euphorbia heterophylla* leaf extract: A recoverable catalyst for reduction of organic dyes. *J Alloys Compd.* 2016;685:258–65.
22. Atarod M, Nasrollahzadeh M, Mohammad Sajadi S. *Euphorbia heterophylla* leaf extract mediated green synthesis of Ag/TiO₂ nanocomposite and investigation of its excellent catalytic activity for reduction of variety of dyes in water. *J Colloid Interface Sci.* 2016;462:272–9.
23. Estomba D, Ladio A, Lozada M. Medicinal wild plant knowledge and gathering patterns in a Mapuche community from North-western Patagonia. *J Ethnopharmacol.* 2006;103(1):109–19.
24. Backhouse N, Delporte C, Apablaza C, Farías M, Goity L, Arrau S, et al. Antinociceptive activity of *Buddleja globosa* (matico) in several models of pain. *J Ethnopharmacol.* 2008;119(1):160–5.
25. Backhouse N, Rosales L, Apablaza C, Goity L, Erazo S, Negrete R, et al. Analgesic, anti-inflammatory and antioxidant properties of *Buddleja globosa*, *Buddlejaceae*. *J Ethnopharmacol.* 2008;116(2):263–9.
26. Sahu K, Kurrey R, Pillai AK. Green synthesis of silver nanoparticles from *Manilkara zapota* leaf extract for the detection of aminoglycoside antibiotics and other applications. *RSC Adv.* 2024;14(32):23240–56.
27. Skiba MI, Vorobyova VI. Synthesis of Silver Nanoparticles Using Orange Peel Extract Prepared by Plasmochemical Extraction Method and Degradation of Methylene Blue under Solar Irradiation. *Adv Mater Sci Eng.* 2019;2019.
28. Saha A, Giri Kumar N, Agarwal S. Silver nanoparticle based hydrogels of Tulsi extracts for tropical drug delivery. *Int J Ayurveda Pharma Res.* 2017;5(1):17–23.
29. Kahrilas GA, Wally LM, Fredrick SJ, Hiskey M, Prieto AL, Owens JE. Microwave-assisted green synthesis of silver nanoparticles using orange peel extract. *ACS Sustain Chem Eng.* 2014;2(3):367–76.
30. Awad MA, Hendi AA, Ortashi KMO, Elradi DFA, Eisa NE, Al-Lahieb LA, et al. Silver nanoparticles biogenic synthesized using an orange peel extract and their use as an anti-bacterial agent. *Int J Phys Sci.* 2014;9(3):34–40.
31. Rizwana H, Alwhibi MS, Al-Judaie RA, Aldehaish HA, Alsaggabi NS. Sunlight-Mediated Green Synthesis of Silver Nanoparticles Using the Berries of *Ribes rubrum* (Red Currants): Characterisation and Evaluation of Their Antifungal and Antibacterial Activities. *Molecules.* 2022;27(7).
32. Bratovic A. Biosynthesis of Green Silver Nanoparticles and Its UV-Vis Characterization. *IJSET Interational J Innov Sci Eng Technol.* 2020;7(7):170–6.

33. Santos EDB, Madalossi NV, Sigoli FA, Mazali IO. Silver nanoparticles: Green synthesis, self-assembled nanostructures and their application as SERS substrates. *New J Chem.* 2015;39(4):2839–46.
34. Alsammarraie FK, Wang W, Zhou P, Mustapha A, Lin M. Green synthesis of silver nanoparticles using turmeric extracts and investigation of their antibacterial activities. *Colloids Surfaces B Biointerfaces.* 2018;171:398–405.
35. Raj S, Chand Mali S, Trivedi R. Green synthesis and characterization of silver nanoparticles using *Enicostemma axillare* (Lam.) leaf extract. *Biochem Biophys Res Commun.* 2018;503(4):2814–9.
36. Mahmudin L, Suharyadi E, Utomo ABS, Abraha K. Optical Properties of Silver Nanoparticles for Surface Plasmon Resonance (SPR)-Based Biosensor Applications. *J Mod Phys.* 2015;06(08):1071–6.
37. Smitha SL, Nissamudeen KM, Philip D, Gopchandran KG. Studies on surface plasmon resonance and photoluminescence of silver nanoparticles. *Spectrochim Acta – Part A Mol Biomol Spectrosc.* 2008;71(1):186–90.
38. Niluxsshun MCD, Masilamani K, Mathiventhan U. Green Synthesis of Silver Nanoparticles from the Extracts of Fruit Peel of *Citrus tangerina*, *Citrus sinensis*, and *Citrus limon* for Antibacterial Activities. *Bioinorg Chem Appl.* 2021;2021.